Use of ultra high performance liquid chromatography with high resolution mass spectrometry to analyze urinary metabolome alterations following acute kidney injury in post-cardiac surgery patients

Yunpeng Bai [a,b,1,2], Huidan Zhang [c,d,e,1], Zheng Wu [d,f,1], Sumei Huang [a,g], Zhidan Luo [a], Kunyong Wu [a,g], Linhui Hu [a,b], Chunbo Chen [b,2,*]

[a] Center of Scientific Research, Maoming People's Hospital, Maoming 525000, China
[b] Department of Critical Care Medicine, Maoming People's Hospital, Maoming 525000, China
[c] Department of Intensive Care Unit of Cardiovascular Surgery, Guangdong Cardiovascular Institute, Guangdong Provincial People's Hospital, Guangdong Academy of Medical Sciences, Guangzhou 510080, China
[d] Department of Critical Care Medicine, Guangdong Provincial People's Hospital, Guangdong Academy of Medical Sciences, Guangzhou 510080, China
[e] School of Medicine, South China University of Technology, Guangzhou 510006, China
[f] School of Biology and Biological Engineering, South China University of Technology, Guangzhou 510006, China
[g] Biological Resource Center of Maoming People's Hospital, Maoming 525000, China

ARTICLE INFO

ABSTRACT

Background: Cardiac surgery-associated acute kidney injury (AKI) can increase the mortality and morbidity, and the incidence of chronic kidney disease, in critically ill survivors. The purpose of this research was to investigate possible links between urinary metabolic changes and cardiac surgery-associated AKI.

Methods: Using ultra-high-performance liquid chromatography coupled with Q-Exactive Orbitrap mass spectrometry, non-targeted metabolomics was performed on urinary samples collected from groups of patients with cardiac surgery-associated AKI at different time points, including Before_AKI (uninjured kidney), AKI_Day1 (injured kidney) and AKI_Day14 (recovered kidney) groups. The data among the three groups were analyzed by combining multivariate and univariate statistical methods, and urine metabolites related to AKI in patients after cardiac surgery were screened. Altered metabolic pathways associated with cardiac surgery-induced AKI were identified by examining the Kyoto Encyclopedia of Genes and Genomes database.

Results: The secreted urinary metabolome of the injured kidney can be well separated from the urine metabolomes of uninjured or recovered patients using multivariate and univariate statistical analyses. However, urine samples from the AKI_Day14 and Before_AKI groups cannot be distinguished using either of the two statistical analyses. Nearly 4000 urinary metabolites were identified through bioinformatics methods at Annotation Levels 1–4. Several of these differential metabolites may also perform essential biological functions. Differential analysis of the urinary metabolome among groups was also performed to provide potential prognostic indicators and changes in signalling pathways. Compared with the uninjured kidney group, the patients with cardiac surgery-associated AKI displayed dramatic changes in renal metabolism, including sulphur metabolism and amino acid metabolism.

Conclusions: Urinary metabolite disorder was observed in patients with cardiac surgery-associated AKI due to ischaemia and medical treatment, and the recovered patients' kidneys were able to return to normal. This work provides data on urine metabolite markers and essential resources for further research on AKI.

Introduction

Acute kidney injury (AKI), a syndrome characterised by abrupt deterioration of renal function, is a common complication of cardiac surgery, particularly among critically ill patients [1,2]. AKI may lead to the imbalance of excretory metabolites in the kidney and impairment or loss of the ability to regulate electrolytes and acid-base balance. AKI is also an important risk factor for chronic kidney disease or chronic renal dysfunction, which can accelerate progression to chronic renal failure (CRF) and death [3,4]. Hence, AKI has been regarded as a 'global health alert' and presents an alarming burden with a high incidence and independent impact on prognosis. At present, AKI is diagnosed by increased serum creatinine (sCr) level and decreased urine volume [5]. However, these are not early diagnostic indicators of AKI because the sCr level and urine volume often change only after renal dysfunction has been determined [6]. Therefore, the discovery of biomarkers that can be predictive or provide early diagnosis of AKI has become a research hotspot recently.

As a sensitive indicator of renal tubular and glomerular injury, quantitative proteinuria spectrum has consistently been the focus of predicting nephrotic syndrome, which can also reflect systemic vascular inflammation and endothelial dysfunction [7–9]. Recent studies have associated serum/urine levels of cystatin C with other factors to reflect the glomerular filtration rate [10–13]. Neutrophil gelatinase-associated lipocalin (NGAL), kidney injury molecule-1 (KIM-1), and liver type fatty acid binding protein (L-FABP) were measured to investigate the relationship between inflammatory factors and renal tubular epithelial cell damage [14–17]. The factors for inflammation include urinary interleukin-18 (IL-18) and chemokine activated protein (C-X-C motif chemokine ligand 10), and those for cell cycle arrest comprise urinary insulin-like growth factor binding protein-7 (IGFBP7) and tissue inhibitor of metalloproteinase-2 (TIMP-2) [18]. Complementary to these studies, we previously identified and verified urinary angiotensinogen (uAGT) [19] and urinary matrix metalloproteinase-7 (uMMP-7) [20] as the main altered proteins in response to AKI to promote the clinical application of AKI biomarkers.

Metabolomics is the study of metabolic profiles in a biological system; it can offer potential mechanisms in physiological and pathological states [21]. Changes in metabolite levels are the natural results of the onset and prognosis of numerous diseases because they are normally reflected in biological fluids before the appearance of clinical symptoms [22]. Given its great stability and species independence, metabolomics is a reliable method to identify novel biomarkers for the early detection of nephrotoxicity compared with protein-based methods [23]. As a non-invasive sample source, urine analysis is an attractive option for metabolome biomarker discovery because urine samples can be readily obtained in large quantities with expected participant compliance and low risk of infection to researchers [24,25]. Furthermore, concentrations of renal metabolites in urine are usually higher than those in plasma; thus, urine metabolomics can provide an abundant matrix for predicting the development of nephropathy [26,27].

Urine can contain the whole end products of renal metabolism; thus, the urinary metabolome has been used to predict the development of diabetic nephropathy [28,29] and evaluate the impact of AKI on different developmental stages of preterm neonates and the degree of renal injury under environmental exposure [30]. In this study, we performed the untargeted metabolomics of urine samples collected from a cohort of patients with AKI after cardiac surgery at different time points. The results of this study help elucidate the mechanisms of cardiac surgery-associated AKI and visualise the dynamic progress *via* the urinary metabolome.

Materials and methods

Chemicals and reagents

MS-grade acetonitrile (ACN) and methanol (MeOH) were purchased from Thermo Fisher Scientific, USA. Formic acid was obtained from DIMKA, and ammonium formate was purchased from Fluka (Honeywell Fluka, USA). Ultrapure water was filtered through the Milli-Q system (Millipore, Billerica, MA). The internal standard (IS) mixture contained L-Leucine-d3 (Toronto Research Chemicals, TRC), L-Phenylalanine (^{13}C9, 99%) (Cambridge Isotope Laboratories, CIL), L-Tryptophan-d5 (TRC), Progesterone-2,3,4-^{13}C3 (Sigma).

Patients and sample preparation

This research has been carried out in accordance with the World Medical Association Declaration of Helsinki and approved by the Maoming People's Hospital Ethics Committee. Written informed consents were obtained from the patients before cardiac surgery. AKI was defined in accordance with the KDIGO Clinical Practice Guidelines based on serum creatinine criteria [31], and six male patients with cardiac surgery were enrolled in the study after the diagnosis of AKI. Spot urine samples were collected at three time points, Before_AKI, AKI_Day1 (AKI just occurred) and AKI_Day14 (the rehabilitation of AKI), and were used to compare the changes in urinary metabolic profiles. Serum creatinine was measured after cardiac surgery and at least twice a day during the first 3 days and daily, thereafter. The basic information of patients, including age, gender, Body Mass Index (BMI) and sCr levels at different time points of AKI, is displayed in Table 1.

Urinary metabolite extraction was primarily performed according to previously reported methods [32,33]. In short, 100 μL samples were diluted by directly adding 300 μL of precooled methanol and acetonitrile (2:1, *v/v*) with 10 μL IS mixture. The concentration of each IS was 100 μg/mL, and the solvent system for IS mixture was aqueous methanol (1:1, *v/v*). After vortexing for 1 min and incubating at −20 °C for 2 h, samples were centrifuged at 4,000 *g* for 20 min, and then the supernatant was transferred for vacuum freeze drying. The metabolites were resuspended in 150 μL of 50% aqueous methanol solution and centrifuged at 4,000 *g* for 30 min. The supernatants were transferred to autosampler vials for Ultra High Performance Liquid Chromatography-High Resolution Mass Spectrometry (UHPLC-HRMS) analysis, and 10 μL of each sample was mixed into the quality control (QC) samples to evaluate the repeatability and stability of the whole Liquid Chromatography-Mass Spectrometry (LC-MS) process.

Table 1
Basic information of six AKI patients after cardiac surgery.

No.	Age	Sex	BMI	sCr (μmol/L)		
				Before_AKI	AKI_Day1	AKI_Day14
1	60	Male	20.70	132.2	160.9	96.4
2	53	Male	26.99	80.2	125.0	74.5
3	69	Male	28.26	115.6	205.5	110.7
4	63	Male	20.76	97.0	127.6	118.5
5	46	Male	24.61	112.7	140.7	79.1
6	23	Male	17.42	72.6	154.7	104.2

UHPLC-HRMS measurement of urinary metabolites

The samples were analyzed on a Waters 2D UHPLC (Waters, USA), coupled to a Q-Exactive™ benchtop Orbitrap mass spectrometer (Thermo Fisher Scientific, USA) with a heated electrospray ionization (HESI) source and controlled by the Xcalibur 2.3 software program (Thermo Fisher Scientific, Waltham, MA, USA). Chromatographic separation was performed on a Waters ACQUITY UHPLC BEH C18 column (1.7 μm, 2.1 mm × 100 mm, Waters, USA), the flow rate was 0.35 mL/min, the injection volume was 5 μL, and the column temperature was maintained at 45 °C. The mobile phase for positive ion mode consisted of (A) 0.1% formic acid aqueous and (B) methanol with 0.1% formic acid, while the mobile phase for negative mode consisted of (A) 10 mM aqueous ammonium formate and (B) 95% methanol with 10 mM ammonium formate. Linear gradient was as follows: 0–1 min, 2% B; 1–9 min, 2% − 98% B; 9–12 min, 98% B; 12–12.1 min, 98% – 2% B; 12.1–15 min, 2% B.

The mass spectrometric settings were set as follows: spray voltage, 3.8 kV for positive-ion mode and 3.2 kV for negative-ion mode; sheath gas flow rate, 40 arbitrary units (arb); aux gas flow rate, 10 arb; aux gas heater temperature, 350 °C; capillary temperature, 320 °C. The full scan range was set as 70–1050 *m/z* Fourier transform mass spectrometry (FTMS) scan event with the resolution of 70,000, the automatic gain control (AGC) target of 3e6, and maximum ion injection time (max IT) of 100 ms. Top 3 precursors were selected for subsequent MS/MS fragmentation with a maximum ion injection time of 50 ms, a resolution at 30,000 and AGC target of 1e5. The stepped normalized collision energy (NCE) was set at 20, 40 and 60 eV. In order to provide more reliable experimental results and reduce the systematic error, the samples were randomly ordered and one QC sample was interspersed for every 10 samples.

Metabolite identification and statistical analysis

The acquired mass spectrometry data (raw files) obtained from UHPLC-HRMS were imported into Compound Discoverer 3.1 (Thermo Fisher Scientific, USA) for data processing, including peak extraction, retention time (RT) correction, additive ion pooling, missing value filling, background peak labeling and metabolite identification. In addition, the results of metabolite identification were also integrated with several other databases, such as BGI library (BGI inhouse-developed standard library), mzCloud and ChemSpider (HMDB, KEGG, LipidMaps). The original data exported by Compound Discoverer 3.1 was imported into metaX for data preprocessing and subsequent analysis [34]. The data preprocessing content includes: (1) normalize the data using the Probabilistic Quotient Normalization (PQN) [35] to obtain the relative peak area; (2) correct the batch effect using Quality control-based robust LOESS signal correction (QC-RLSC) [32]; (3) calculate the Coefficient of Variation (CV) of the relative peak area in all QC samples, and delete the compounds with CV greater than 30%.

Log2 logarithmic transformation and Pareto scaling with mean centering for normalization were used to calculate the multivariate statistical analysis between groups, including unsupervised principal component analysis (PCA) for the overall distribution and supervised partial least squares discriminant analysis (PLS-DA) with 7-fold cross validation for the differential urinary metabolites. Two hundred response permutation testing (RPT) was performed to avoid model overfitting, and the variable importance in the projection (VIP) of each metabolite was obtained. The univariate analyses were also performed with Fold-Change analysis (FC) and T-test (Student's T-test). FC-value, p-value and q-value (t.test_p.value_BHcorrect) were separately obtained by FC analysis, T-test and False Discovery Rate (FDR) correction. For differential metabolites, with log2 transformed and z-score normalized, hierarchical cluster was used as the clustering algorithm and the distance calculation was performed in Euclidean distance. Furthermore, metabolic pathway enrichment analysis of differential metabolites was carried out based on the Kyoto Encyclopedia of Genes and Genomes (KEGG) database. Metabolic pathways with a p-value < 0.05 were significantly enriched by differential metabolites.

Results

Patients and analytical performance of the MS instrument

To improve the metabolic coverage, we used positive-ion and negative-ion scan modes for the untargeted metabolomics of urine samples from patients with AKI after cardiac surgery at different time points using Q Exactive HRMS coupled with an UHPLC system. The urine samples were collected at Maoming People's Hospital from patients with AKI who were confirmed by the sCr test. The samples from each patient with AKI were divided into three groups to compare the urinary metabolome at different stages of AKI: Before_AKI (uninjured kidney), AKI_Day1 (injured kidney) and AKI_Day14 (recovered kidney). Six male patients with AKI, including three patients aged 60–70 years old, one in his fifties, one in his forties and one in his twenties, were enrolled for the analysis of urinary metabolic profiles. Compared with that of the Before_AKI group, the sCr level of the AKI_Day1 group significantly increased, and that of the AKI_Day14 group returned to normal.

QC samples were regularly inserted into every ten samples of the analytical batch to evaluate the reproducibility and stability of the analytical system. As shown in Figure S1, ten QC samples from each group were closely aggregated in the principal component analysis (Figure S1A for the positive-ion mode and Figure S1B for the negative-ion mode), indicating that the instrument was satisfactory and the MS signal was stable during sample detection. As for QC samples, the relative standard deviation (RSD) of ≤ 30% from the integrated peak areas was the exclusion criterion, and the MS datasets were qualified when the RSD_Ratio (RSD_30_number/total ion number) was ≥ 60%. In positive-ion mode, 18,641 ion molecules were detected and 16,471 were RSD_30_number of the QC samples. Thus, the RSD_Ratio was equal to 0.884 (>60%, Figure S1C), which demonstrated the high-quality data of the QC samples during the running process. Figure S1D shows that the RSD_ Ratio was 0.885 in the QC samples in the negative-ion mode. Therefore, the results suggested that the urinary metabolic characteristics were reproducible and reliable in the MS experiments.

Metabolite identification and functional annotation

Urine metabolites were annotated with five confidence levels on the basis of the matching information for identification, such as MS1 molecular weight, MS2 fragment ion spectra, column RT and the presence or absence of reference standards. Level 1: Identified results were from standard libraries with the matching of MS1, MS2 spectra and RT. Level 2: Identified results were from standard libraries. Except for RT information, MS1 and MS2 spectra can exactly match the libraries. Level 3: Identified results were from database libraries, MS1 can match the theoretical values, and MS2 spectra can match the predicted MS2 spectra from the database. Level 4: Identified results were from database libraries, and only MS1 can match the theoretical values. Level 5: The molecular formula can match the accurate molecular weight, but no matching reference can be found in the database. The reliability of Level 1 to Level 5 decreased in turn. In the positive-ion mode, 45 (Level 1), 441 (Level 2), 451 (Level 3) and 3100 (Level 4) unique metabolite molecules were identified from the 16,471 detected ions *via* Compound Discoverer software (Table S1), and they refer to the addition of H^+, NH_4^+, Na^+, K^+ and so on. Meanwhile, 12 (Level 1), 224 (Level 2), 176 (Level 3) and 2126 (Level 4) unique metabolites were identified by the software from 10,098 detected ions in the negative-ion mode (Table S2), and they refer to the negative ions of −H, +Cl and so on. Furthermore, two examples of identified metabolites (taurine in negative-ion mode and creatine in positive-ion mode), including those obtained in tandem
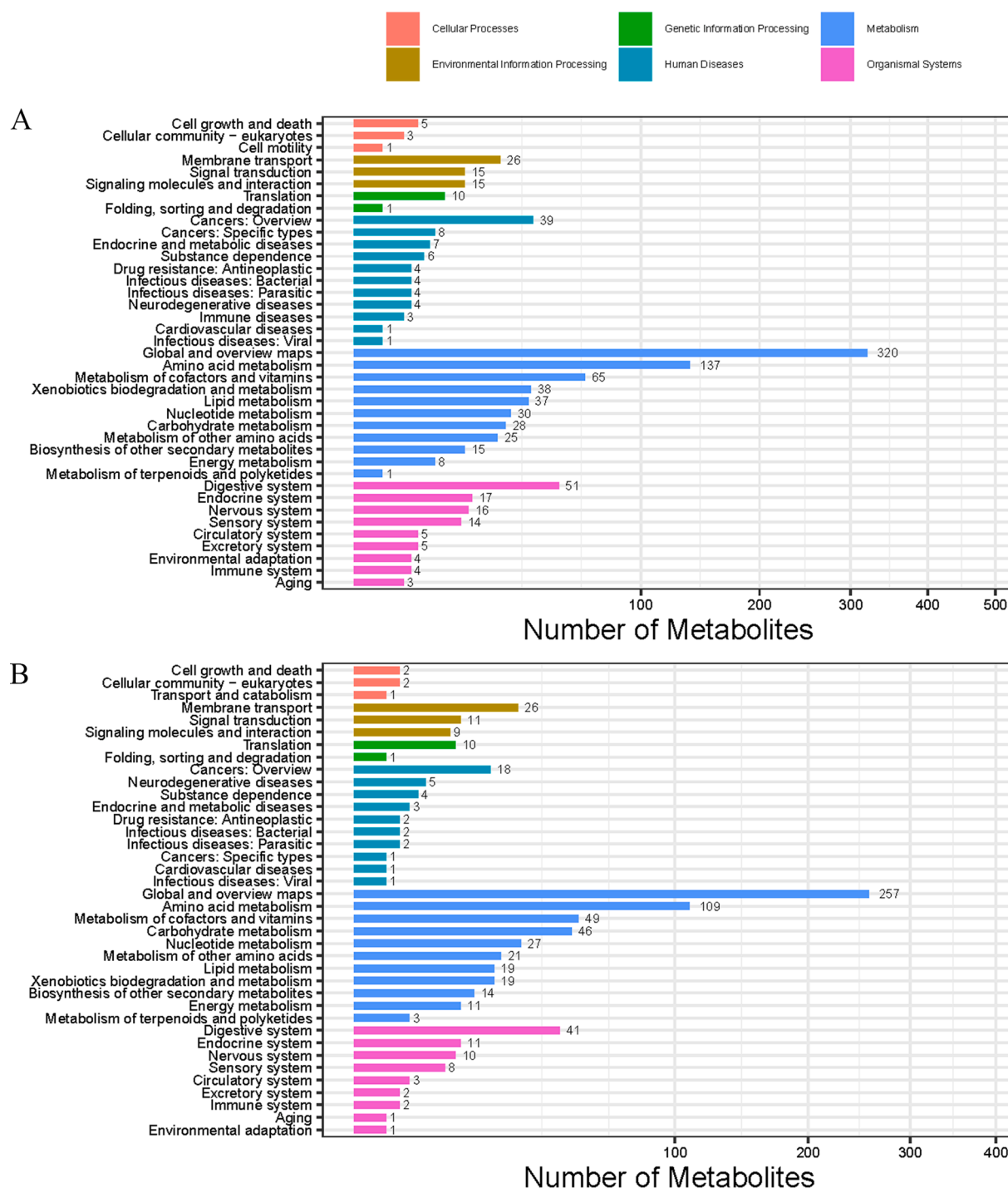
Fig. 1. Functional annotations of urinary metabolites by the KEGG database. (A) of the positive-ion mode, (B) of the negative-ion mode. The vertical axis, horizontal axis and different colours correspond to the functional annotation, the number of urinary metabolites and different categories.

MS and fragmented pathways, are displayed in the Supplementary Materials.

Statistical analysis was performed on the classification and functional annotation of metabolites after data pre-treatment. Figure S2 shows the statistical chart of metabolic classifications and the corresponding number of identified metabolic molecules in the positive- and negative-ion modes, respectively. The defined metabolites can be classified into compounds with biological roles, lipids, phytochemical compounds and others; these compounds included benzene derivatives, amino acid analogues, organic acids, carbohydrates, amines, indoles, nucleic acids, vitamins and so on. 'Others' meant that classification

information was the remaining categories, and the identification results without classification information were not included in statistics. Functional annotations of the identified metabolites were performed by KEGG analysis to investigate the main biochemical characteristics and signal transduction pathways. Fig. 1 shows the number of metabolites identified in each type of metabolic pathway, which may refer to cell processes, genetic information processing, metabolism, environmental information processing, human diseases and organismal systems.

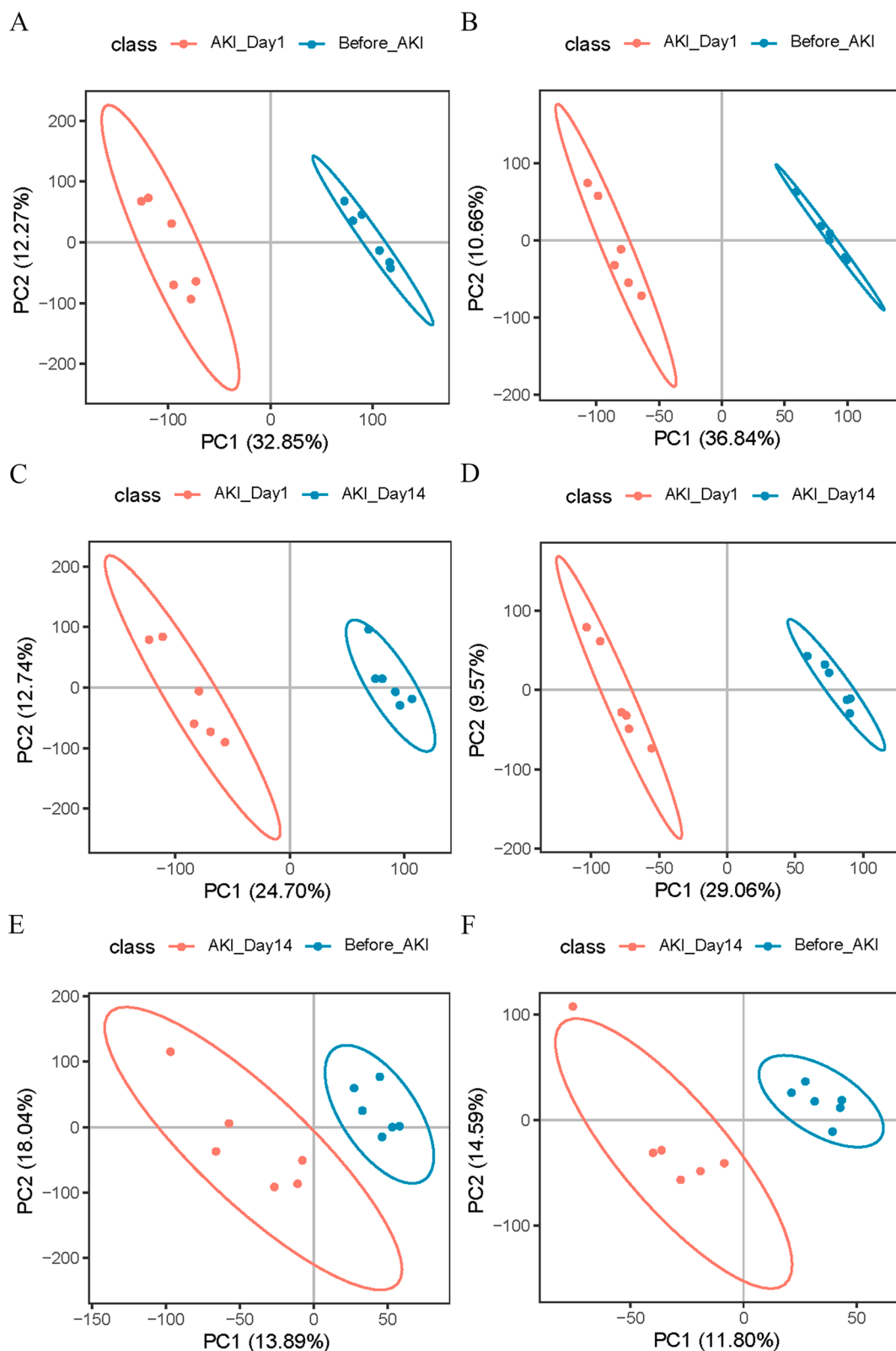**Fig. 2.** Plot of AKI patients' PLS-DA scores using Pareto scaling with mean centring. (A) Before_AKI vs. AKI_Day1 in the positive-ion mode, (B) Before_AKI vs. AKI_Day1 in the negative-ion mode, (C) AKI_Day1 vs. AKI_Day14 in the positive-ion mode, (D) AKI_Day1 vs. AKI_Day14 in the negative-ion mode, (E) Before_AKI vs. AKI_Day14 in the positive-ion mode (over-fitted), (F) Before_AKI vs. AKI_Day14 in the negative-ion mode (over-fitted).

Table 2

PLS-DA mode parameters among the groups.

Group	MS mode	principal component No.	R^2Y(cum)	Q^2(cum)	R^2	Q^2
Before_AKI: AKI_Day1	positive	3	1	0.87	(0.0,0.98)	(0.0,−0.73)
	negative	3	1	0.94	(0.0,0.98)	(0.0,−0.81)
AKI_Day1: AKI_Day14	positive	3	1	0.81	(0.0,0.99)	(0.0,−0.72)
	negative	3	1	0.9	(0.0,0.99)	(0.0,−0.67)
Before_AKI: AKI_Day14	positive	3	0.99	−0.41	(0.0,0.99)	(0.0,−0.36)
	negative	3	0.99	−0.65	(0.0,0.99)	(0.0,−0.34)

Table 3

Overview of differential urinary metabolites at different AKI time points.

Group	MS mode	differential metabolites	up-regualted	down-regulated
Before_AKI: AKI_Day1	positive	3049	1438	1611
	negative	2091	921	1170
AKI_Day1: AKI_Day14	positive	1824	1312	512
	negative	1424	923	501
Before_AKI: AKI_Day14	positive	3	0	3
	negative	0	0	0

Differential screening and statistical analysis of urinary metabolites

The urinary metabolite differences among different groups were compared using the score plots of PLS-DA to investigate the cluster data before and after AKI (Fig. 2A/B for Before_AKI: AKI_Day1 in the positive/negative-ion mode, Fig. 2C/D for AKI_Day1: AKI_Day14 in the positive/negative-ion mode, and Fig. 2E/F for Before_AKI: AKI_Day14 in the positive/negative-ion mode). PLS-DA models were established after the log2 logarithmic transformation and the Pareto scaling method. Seven-fold cross-validation was performed when building the models, and 200 RPTs were performed on PLS-DA to assess the model quality. As shown in Table 2, several parameters were used to evaluate the PLS-DA models: R^2Y(cum) is the interpretation rate for the Y matrix; Q^2(cum) is the predictive capability; R^2 and Q^2 are the intercepts of the Y-axis for the regression line during permutation experiments. When the values of R^2Y(cum) and Q^2(cum) are close to 1, the models are stable and reliable. An evident clustering trend was observed in the AKI_Day1 group with acceptable R^2Y(cum) and Q^2(cum), which indicated distinct urinary metabolic profiles due to injured kidneys. Since the values of Q^2(cum) were<0.5, however, the PLS-DA models between Before_AKI and AKI_Day14 were over-fitted in positive- and negative-ion modes. Multivariate and univariate analyses were performed to screen the differential metabolic molecules between groups. Changes in urinary metabolites were determined by VIP > 1.0 combined with a fold change (FC) and false discovery rate (FDR) correction; FC $\geq$ 1.2 or $\leq$ 0.83 and $q < 0.05$ were set as the level of statistical significance (Table 3).

In accordance with the above criteria, the numbers of differential metabolites were 3049 and 2091 for Before_AKI versus AKI_Day1 in the positive- and negative-ion modes (Table S3) and 1824 and 1424 for AKI_Day1 versus AKI_Day14 in each ion mode (Table S4). For the comparison of Before_AKI and AKI_Day14 groups, however, the number of differential metabolites was nearly zero, regardless of the ion mode. Thus, the differential analyses between these two groups were not performed in the following statistical analysis. The urinary differential metabolites were visualised through the volcano plot in Fig. 3, which indicated that univariate analysis was also suitable for the UHPLC-HRMS data. Figure S3 displays the cluster analysis of these differential metabolites. Metabolic pathway enrichment analysis of differential metabolites was performed on the basis of the KEGG database in Table 4 and Fig. 4. Metabolic pathways with $p < 0.05$ were significantly enriched by differential metabolites, which demonstrated that differential metabolites were particularly enriched in amino acid metabolism and biosynthesis, sulphur metabolism, ABC transporters, bile secretion and so on.

Discussion

This study aimed to generate a high-quality resource of urinary metabolite datasets from patients with AKI after cardiac surgery and to compare alterations of urinary metabolite profiles, which may reflect kidney status. Q Exactive HRMS can sensitively and accurately determine the composition of the precursors and product metabolite ions. In addition, BGI Library is an in-house developed standard database, including RT, MS1 spectra and MS2 spectra of all standards. mzCloud is Thermo's high-resolution tandem MS cloud database containing a high-resolution and accurate MS^n spectra library of tens of thousands of compounds. All MS data in mzCloud are measured by standards and subject to strict manual corrections. As a plug-in for the Compound Discoverer software, Chemspider can provide online compound identification from HMDB, KEGG, LipidMaps and so on. After the metabolic feature extraction and alignment, the full-scan MS results in the UHPLC-HRMS analysis were used in the multivariate/univariate statistical analysis to extract statistically significant urinary metabolites among groups. Endogenous differential metabolites as potential biomarkers were mapped onto metabolic pathways to reveal the possible pathway dysregulation for AKI after cardiac surgery.

As a relatively frequent complication of cardiac surgery, AKI occurs in approximately 4%–9% of surgical patients and has short- and long-term survival implications [36]. Considering the absence of effective treatments for AKI, clinicians often focus on prevention and risk factor management to reduce AKI rates [37,38]. Therefore, efforts have been exerted to identify biomarkers relevant to cardiac surgery-associated AKI, which include renal/non-renal tubule-associated biomarkers, cardiac functional biomarkers and inflammation biomarkers, with high specificity and sensitivity [39]. For example, we have previously shown that uMMP-7 levels can faithfully reflect renal Wnt/β-catenin activity [40] and be used as a non-invasive biomarker for the early prediction of AKI after cardiac surgery [20]. Meanwhile, the metabolic alterations of plasma in patients who underwent cardiac surgery were also investigated to reflect the systematic responses and identify metabolites prognostic of AKI [41]. Patients with mild AKI also showed metabolic changes similar to those of patients with severe AKI, which revealed the potential role of metabolic analysis in the assessment of early renal injury [42]. Furthermore, urinary metabolome has become an important field for the discovery of non-invasive biomarkers; it can also be used to detect subtle metabolic discrepancies caused by specific diseases or treatment interventions [25].

The altered urinary metabolome revealed that sulphur metabolism was significantly disrupted in patients with AKI after cardiac surgery. Methane sulphonic acid and taurine are involved in sulphur metabolism, and taurine is an important component of membrane stability and cell protection, antioxidant and anti-inflammatory effects, calcium homeostasis regulation and nerve regulation [43]. In the study of AKI models, taurine therapy can improve oxidative stress and histopathological kidney damage in rats [44] and inhibit the production of inflammatory cytokines and the activity of caspase-3 and caspase-9 to ameliorate
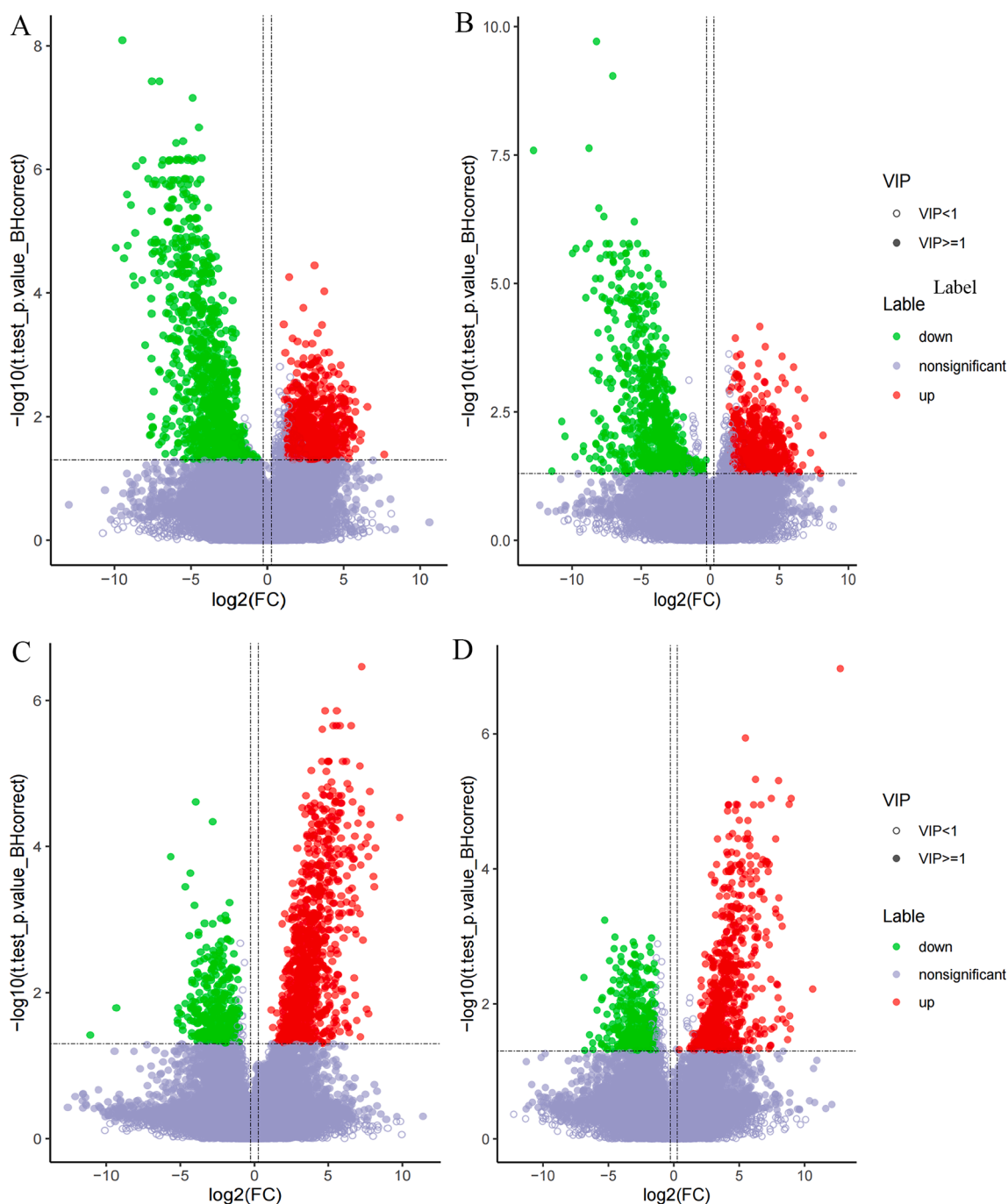
Fig. 3. Volcano Plot for visually displaying the differential metabolic compounds. (A) Before_AKI vs. AKI_Day1 in the positive-ion mode, (B) Before_AKI vs. AKI_Day1 in the negative-ion mode, (C) AKI_Day1 vs. AKI_Day14 in the positive-ion mode, (D) AKI_Day1 vs. AKI_Day14 in the negative-ion mode. The solid circles are the urinary metabolites with variable importance in the projection (VIP) greater than or equal to 1, the hollow circles are the urinary metabolites with VIP<1, the green are the downregulated significantly differential urinary metabolites, the red are the upregulated significantly differential urinary metabolites, and the non-significant urinary metabolites are marked as grey. (For interpretation of the references to colour in this figure legend, the reader is referred to the web version of this article.)

kidney injury [45]. In the current study, the taurine levels of each AKI patient showed differential trends, indicating that taurine levels increased in several patients, but decreased in others during AKI. The taurine levels of the recovered kidney group (AKI_Day14 group) can return to normal conditions compared with those of the uninjured kidney group (Before_AKI group). Therefore, we will simultaneously measure the taurine level in the plasma of individual patients and determine whether it is consistent with the changing trend of urinary taurine. These results suggest that sulphur metabolism plays a vital role in the regulation of the pathophysiology of cardiac surgery-associated AKI.

In addition to sulphur metabolism, the renal metabolism of amino acids, such as tyrosine, tryptophan, phenylalanine, alanine, aspartate and glutamate, was significantly altered in patients with AKI after cardiac surgery. 3-Methylglutaryl carnitine, 1-methylimidazoleacetate and urea (amino acid metabolites) in plasma, along with leucine, histidine and arginine in the metabolic pathways of AKI, can be used as biomarkers to reflect AKI progression [46]. Compared with healthy individuals, patients with AKI had increased levels of acylcarnitines and amino acids (methionine, homocysteine, pyroglutamic acid, asymmetric dimethylarginine and phenylalanine) and decreased serum levels of

Table 4

KEGG enrichment analysis of differential metabolic pathways.

Batch	Pathway	Count	Count. All	Pvalue	Pathway. ID
Before_AKI/ AKI_Day1	Sulfur metabolism	5	33	1.09E-04	map00920
	Alanine, aspartate and glutamate metabolism	4	28	6.91E-04	map00250
	Cysteine and methionine metabolism	5	61	1.96E-03	map00270
	Central carbon metabolism in cancer	4	37	2.01E-03	map05230
	ABC transporters	7	124	2.31E-03	map02010
	Bile secretion	6	97	2.99E-03	map04976
	Protein digestion and absorption	4	47	4.85E-03	map04974
	Tyrosine metabolism	6	78	5.68E-03	map00350
	Nicotinate and nicotinamide metabolism	4	55	8.47E-03	map00760
	beta-Alanine metabolism	3	32	1.12E-02	map00410
	Biosynthesis of amino acids	6	128	1.13E-02	map01230
	Phenylalanine metabolism	4	60	1.14E-02	map00360
	Phenylalanine, tyrosine and tryptophan biosynthesis	3	35	1.43E-02	map00400
	Parathyroid hormone synthesis, secretion and action	2	10	2.06E-02	map04928
	Prostate cancer	2	11	2.48E-02	map05215
	Metabolic pathways	35	1706	2.52E-02	map01100
	Intestinal immune network for IgA production	1	2	2.90E-02	map04672
	Cortisol synthesis and secretion	2	12	2.94E-02	map04927
	Histidine metabolism	3	47	3.12E-02	map00340
	Riboflavin metabolism	2	20	3.40E-02	map00740
	Cushing syndrome	2	13	3.42E-02	map04934
	Tryptophan metabolism	5	81	3.75E-02	map00380
	Aminoacyl-tRNA biosynthesis	3	52	4.03E-02	map00970
	Neuroactive ligand-receptor interaction	3	52	4.03E-02	map04080
	Caffeine metabolism	2	22	4.05E-02	map00232
	Taurine and hypotaurine metabolism	2	22	4.05E-02	map00430
	Small cell lung cancer	1	3	4.32E-02	map05222
	Arginine biosynthesis	2	23	4.40E-02	map00220
	HIF-1 signaling pathway	2	15	4.47E-02	map04066
	Parkinson disease	2	15	4.47E-02	map05012
	Pentose and glucuronate interconversions	3	55	4.64E-02	map00040
		8	128		map01230

Table 4 (*continued*)

Batch	Pathway	Count	Count. All	Pvalue	Pathway. ID
AKI_Day1/ AKI_Day14	Biosynthesis of amino acids			7.43E-05	
	Alanine, aspartate and glutamate metabolism	4	28	2.18E-04	map00250
	Mineral absorption	4	29	2.51E-04	map04978
	Sulfur metabolism	4	33	4.18E-04	map00920
	Central carbon metabolism in cancer	4	37	6.52E-04	map05230
	Protein digestion and absorption	4	47	1.62E-03	map04974
	Arginine biosynthesis	3	23	1.86E-03	map00220
	Aminoacyl-tRNA biosynthesis	4	52	2.36E-03	map00970
	Bile secretion	5	97	3.98E-03	map04976
	Cysteine and methionine metabolism	4	61	4.21E-03	map00270
	Phenylalanine, tyrosine and tryptophan biosynthesis	3	35	1.25E-02	map00400
	Glycine, serine and threonine metabolism	3	50	1.66E-02	map00260
	Nicotinate and nicotinamide metabolism	3	55	2.14E-02	map00760
	Valine, leucine and isoleucine biosynthesis	2	23	2.51E-02	map00290
	Phenylalanine metabolism	3	60	2.69E-02	map00360
	mTOR signaling pathway	1	4	4.24E-02	map04150
	ABC transporters	4	124	4.51E-02	map02010

arginine and several lysophosphatidylcholines [47]. In addition, the metabolomic analysis showed that tryptophan, phenylalanine, lyso-phosphatidylcholine, creatinine and canine urea can be used as serum biomarkers of modelling with CRF, which indicated that the metabolism of amino acids and phospholipids was abnormal in CRF rats [48]. However, a major limitation of the study was the small sample size (six patients). Thus, individual factors, such as underlying diseases, may affect the results of statistical analysis. To further compare the urinary proteins, we also conducted the semi-quantification of urinary proteins on uninjured/injured kidneys using the Bradford method. Through the semi-quantified results for urinary proteins (Supplementary Materials), the protein levels in urine samples significantly increased for all AKI patients, but a wide range of urinary proteins due to patient demographics (e.g., age, BMI, etc) was observed. Thus, the variations in urinary metabolome are less affected by patient demographics for AKI patients. Although the sample size was relatively small during the comparison, this work can provide valuable knowledge of AKI-related urinary biomarkers and metabolic pathways for potential therapeutic targets. Future studies of the urinary metabolome may need additional time points in multicentre cohorts for rigorous algorithm analysis to minimize batch effects and confirm our results [49].

Conclusions

Our results indicate that renal metabolism, including sulphur metabolism and amino acid metabolism, dramatically change in patients with
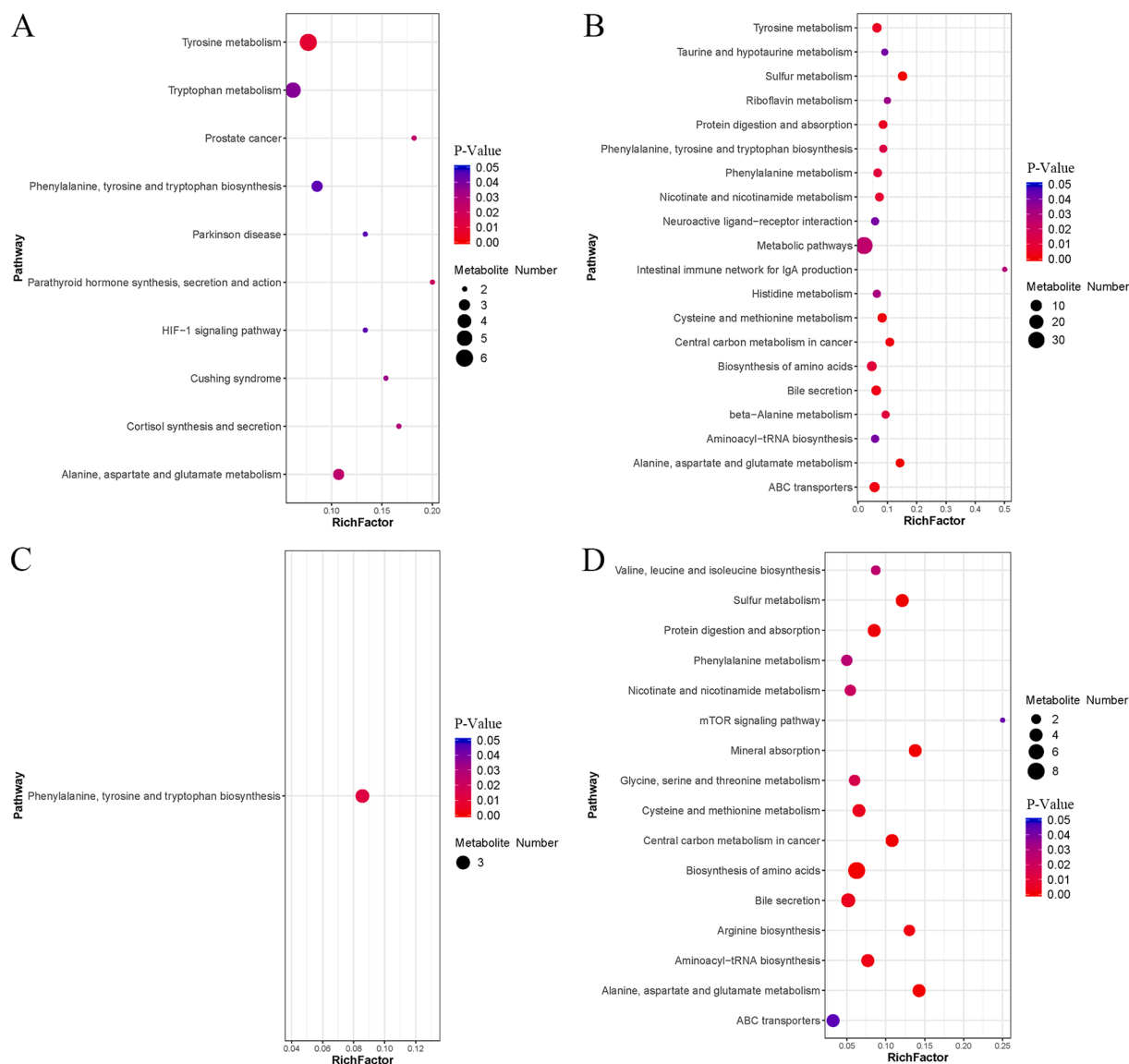
Fig. 4. Metabolomics KEGG pathway enrichment analysis of patients with AKI. (A) Before_AKI vs. AKI_Day1 in the positive-ion mode, (B) Before_AKI vs. AKI_Day1 in the negative-ion mode, (C) AKI_Day1 vs. AKI_Day14 in the positive-ion mode, (D) AKI_Day1 vs. AKI_Day14 in the negative-ion mode. The size of bubbles represents the number of counts, and the colour of bubbles represents the raw *p*-value.

AKI. Such an MS-based metabolomics strategy can help in obtaining highly valuable resources to improve the understanding of the altered metabolism of patients with AKI after cardiac surgery. This study will broaden our knowledge about urinary metabolite profiles reflecting the renal status, accelerate the identification of disease biomarkers and provide new insights into the development of preventive treatments for cardiac surgery-associated AKI.

Data availability

The mass spectrometry data have been deposited to iProX (ww.iprox.org) with ID IPX0003038000 and the ProteomeXchange Consortium (http://proteomecentral.proteomexchange.org) *via* the iProX partner repository [50] with the dataset identifier PXD025917.

Declaration of Competing Interest

The authors declare that they have no known competing financial interests or personal relationships that could have appeared to influence the work reported in this paper.

Appendix A. Supplementary data

Supplementary data to this article can be found online at https://doi.org/10.1016/j.jmsacl.2022.02.003.

References

[1] N.H. Lameire, A. Bagga, D. Cruz, J. De Maeseneer, Z. Endre, J.A. Kellum, K.D. Liu, R.L. Mehta, N. Pannu, W. Van Biesen, R. Vanholder, Acute kidney injury: an increasing global concern, Lancet 382 (2013) 170–179.

[2] R. Santos, A. Carvalho, L. Peres, C. Ronco, E. Macedo, An epidemiologic overview of acute kidney injury in intensive care units, Rev. Assoc. Med. Bras. 65 (2019) (1992) 1094–1101.

[3] S.M. Bagshaw, The long-term outcome after acute renal failure, Curr. Opin. Crit. Care 12 (6) (2006) 561–566.

[4] O. Rewa, S.M. Bagshaw, Acute kidney injury-epidemiology, outcomes and economics, Nat. Rev. Nephrol. 10 (4) (2014) 193–207.

[5] J. Ho, M. Reslerova, B. Gali, P.W. Nickerson, D.N. Rush, M.M. Sood, J. Bueti, P. Komenda, E. Pascoe, R.C. Arora, C. Rigatto, Serum creatinine measurement immediately after cardiac surgery and prediction of acute kidney injury, Am. J. Kidney Dis. 59 (2) (2012) 196–201.

[6] J.A. Kellum, N. Lameire, Diagnosis, evaluation, and management of acute kidney injury: a KDIGO summary (Part 1), Crit. Care 17 (2013) 204.

[7] M.R. Bennett, P. Devarajan, Proteomic analysis of acute kidney injury: biomarkers to mechanisms, Proteomics Clin. Appl. 5 (2011) 67–77.

[8] M. Fang, S. Liu, Y. Zhou, Y. Deng, Q. Yin, L. Hu, X. Ouyang, Y. Hou, C. Chen, Circular RNA involved in the protective effect of losartan on ischemia and reperfusion induced acute kidney injury in rat model, Am. J. Transl. Res. 11 (2019) 1129–1144.

[9] Y. Wu, W. Peng, R.u. Wei, Y. Zhou, M. Fang, S. Liu, Y. Deng, Q.i. Yin, X. Ouyang, L. Hu, Y. Hou, C. Chen, Rat mRNA expression profiles associated with inhibition of ischemic acute kidney injury by losartan, Biosci. Rep. 39 (4) (2019).

[10] D. Zhang, L. Gao, H. Ye, R. Chi, L. Wang, L. Hu, X. Ouyang, Y. Hou, Y. Deng, Y. Long, W. Xiong, C. Chen, Impact of thyroid function on cystatin C in detecting acute kidney injury: a prospective, observational study, BMC Nephrol. 20 (2019) 41.

[11] S. Liang, M. Shi, Y. Bai, Y. Deng, M. Fang, J. Li, Y. Wu, W. Peng, Y. Hou, H. Fang, H. Zhang, C. Chen, The effect of glucocorticoids on serum cystatin C in identifying acute kidney injury: a propensity-matched cohort study, BMC Nephrol. 21 (2020) 519.

[12] Y. Deng, L. Wang, Y. Hou, J. Ma, R. Chi, H. Ye, Y. Zhai, D. Zhang, L.u. Gao, L. Hu, T. Hou, J. Li, N. Tan, C. Chen, The influence of glycemic status on the performance of cystatin C for acute kidney injury detection in the critically ill, Ren. Fail. 41 (1) (2019) 139–149.

[13] Y. Deng, J. Yuan, R. Chi, H. Ye, D. Zhou, S. Wang, C. Mai, Z. Nie, L. Wang, Y. Zhai, L. Gao, D. Zhang, L. Hu, Y. Deng, C. Chen, The incidence, risk factors and outcomes of postoperative acute kidney injury in neurosurgical critically Ill patients, Sci. Rep. 7 (2017) 4245.

[14] Y. Deng, J. Ma, Y. Hou, D. Zhou, T. Hou, J. Li, S. Liang, N. Tan, C. Chen, Combining serum cystatin C and urinary N-acetyl-beta-D-glucosaminidase improves the precision for acute kidney injury diagnosis after resection of intracranial space-occupying lesions, Kidney Blood Press. Res. 45 (1) (2020) 142–156.

[15] Y. Deng, R. Chi, S. Chen, H. Ye, J. Yuan, L. Wang, Y. Zhai, L. Gao, D. Zhang, L. Hu, B. Lv, Y. Long, C. Sun, X. Yang, X. Zou, C. Chen, Evaluation of clinically available renal biomarkers in critically ill adults: a prospective multicenter observational study, Crit. Care 21 (2017) 46.

[16] M. Zdziechowska, A. Gluba-Brzózka, A.R. Poliwczak, B. Franczyk, M. Kidawa, M. Zielinska, J. Rysz, Serum NGAL, KIM-1, IL-18, L-FABP: new biomarkers in the diagnostics of acute kidney injury (AKI) following invasive cardiology procedures, Int. Urol. Nephrol. 52 (2020) 2135–2143.

[17] L. Wang, Y. Deng, Y. Zhai, F. Xu, J. Li, D. Zhang, L. Gao, Y. Hou, X. OuYang, L. Hu, J. Yuan, H. Ye, R. Chi, C. Chen, Impact of blood glucose levels on the accuracy of urinary N-acety-β-D-glucosaminidase for acute kidney injury detection in critically ill adults: a multicenter, prospective, observational study, BMC Nephrol. 20 (2019) 186.

[18] W. Fan, G. Ankawi, J. Zhang, K. Digvijay, D. Giavarina, Y. Yin, C. Ronco, Current understanding and future directions in the application of TIMP-2 and IGFBP7 in AKI clinical practice, Clin. Chem. Lab. Med. 57 (2019) 567–576.

[19] C. Chen, X. Yang, Y. Lei, Y. Zha, H. Liu, C. Ma, J. Tian, P. Chen, T. Yang, F.F. Hou, Urinary biomarkers at the time of AKI diagnosis as predictors of progression of AKI among patients with acute cardiorenal syndrome, Clin. J. Am. Soc. Nephrol. 11 (9) (2016) 1536–1544.

[20] X. Yang, C. Chen, S. Teng, X. Fu, Y. Zha, H. Liu, L.i. Wang, J. Tian, X. Zhang, Y. Liu, J. Nie, F.F. Hou, Urinary matrix metalloproteinase-7 predicts severe AKI and poor outcomes after cardiac surgery, J. Am. Soc. Nephrol. 28 (11) (2017) 3373–3382.

[21] C.H. Johnson, J. Ivanisevic, G. Siuzdak, Metabolomics: beyond biomarkers and towards mechanisms, Nat. Rev. Mol. Cell Biol. 17 (7) (2016) 451–459.

[22] S. Grison, G. Favé, M. Maillot, L. Manens, O. Delissen, E. Blanchardon, N. Banzet, C. Defoort, R. Bott, I. Dublineau, J. Aigueperse, P. Gourmelon, J.-C. Martin, M. Souidi, Metabolomics identifies a biological response to chronic low-dose natural uranium contamination in urine samples, Metabolomics 9 (6) (2013) 1168–1180.

[23] A.J. Won, S. Kim, Y.G. Kim, K.-B. Kim, W.S. Choi, S. Kacew, K.S. Kim, J.H. Jung, B. M. Lee, S. Kim, H.S. Kim, Discovery of urinary metabolomic biomarkers for early detection of acute kidney injury, Mol. BioSyst. 12 (1) (2016) 133–144.

[24] R.C. Miller, E. Brindle, D.J. Holman, J. Shofer, N.A. Klein, M.R. Soules, K. A. O'Connor, Comparison of specific gravity and creatinine for normalizing urinary reproductive hormone concentrations, Clin. Chem. 50 (5) (2004) 924–932.

[25] M.M. Khamis, D.J. Adamko, A. El-Aneed, Mass spectrometric based approaches in urine metabolomics and biomarker discovery, Mass Spectrom. Rev. 36 (2) (2017) 115–134.

[26] M. Martin-Lorenzo, L. Gonzalez-Calero, A. Ramos-Barron, M.D. Sanchez-Niño, C. Gomez-Alamillo, J.M. García-Segura, A. Ortiz, M. Arias, F. Vivanco, G. Alvarez-

Llamas, Urine metabolomics insight into acute kidney injury point to oxidative stress disruptions in energy generation and H(2)S availability, J. Mol. Med. (Berl) 95 (12) (2017) 1399–1409.

[27] K. Kim, P. Aronov, S.O. Zakharkin, D. Anderson, B. Perroud, I.M. Thompson, R. H. Weiss, Urine metabolomics analysis for kidney cancer detection and biomarker discovery, Mol. Cell. Proteomics 8 (3) (2009) 558–570.

[28] C.-J. Chen, W.-L. Liao, C.-T. Chang, Y.-N. Lin, F.-J. Tsai, Identification of urinary metabolite biomarkers of type 2 diabetes nephropathy using an untargeted metabolomic approach, J. Proteome Res. 17 (11) (2018) 3997–4007.

[29] J. Wang, W. Yan, X. Zhou, Y.u. Liu, C. Tang, Y. Peng, H. Liu, L. Sun, Li. Xiao, L. He, Metabolomics window into the role of acute kidney injury after coronary artery bypass grafting in diabetic nephropathy progression, PeerJ 8 (2020) e9111.

[30] K. Mercier, S. McRitchie, W. Pathmasiri, A. Novokhatny, R. Koralkar, D. Askenazi, P.D. Brophy, S. Sumner, Preterm neonatal urinary renal developmental and acute kidney injury metabolomic profiling: an exploratory study, Pediatric Nephrol. 32 (1) (2017) 151–161.

[31] A. Khwaja, KDIGO clinical practice guidelines for acute kidney injury, Nephron Clin. Pract. 120 (4) (2012) c179–c184.

[32] W.B. Dunn, D. Broadhurst, P. Begley, E. Zelena, S. Francis-McIntyre, N. Anderson, M. Brown, J.D. Knowles, A. Halsall, J.N. Haselden, A.W. Nicholls, I.D. Wilson, D. B. Kell, R. Goodacre, Procedures for large-scale metabolic profiling of serum and plasma using gas chromatography and liquid chromatography coupled to mass spectrometry, Nat. Protoc. 6 (7) (2011) 1060–1083.

[33] M.H. Sarafian, M. Gaudin, M.R. Lewis, F.-P. Martin, E. Holmes, J.K. Nicholson, M.-E. Dumas, Objective set of criteria for optimization of sample preparation procedures for ultra-high throughput untargeted blood plasma lipid profiling by ultra performance liquid chromatography-mass spectrometry, Anal. Chem. 86 (12) (2014) 5766–5774.

[34] B. Wen, Z. Mei, C. Zeng, S. Liu, metaX: a flexible and comprehensive software for processing metabolomics data, BMC Bioinf. 18 (2017) 183.

[35] R. Di Guida, J. Engel, J.W. Allwood, R.J. Weber, M.R. Jones, U. Sommer, M. R. Viant, W.B. Dunn, Non-targeted UHPLC-MS metabolomic data processing methods: a comparative investigation of normalisation, missing value imputation, transformation and scaling, Metabolomics 12 (2016) 93.

[36] R.H. Thiele, J.M. Isbell, M.H. Rosner, AKI associated with cardiac surgery, Clin. J. Am. Soc. Nephrol. 10 (3) (2015) 500–514.

[37] U.A. Khan, S.G. Coca, K. Hong, J.L. Koyner, A.X. Garg, C.S. Passik, M. Swaminathan, S. Garwood, U.D. Patel, S. Hashim, M.A. Quantz, C.R. Parikh, Blood transfusions are associated with urinary biomarkers of kidney injury in cardiac surgery, J. Thorac. Cardiovasc. Surg. 148 (2) (2014) 726–732.

[38] M.S. Goepfert, H.P. Richter, E.C. Zu, J. Gruetzmacher, E. Rafflenbeul, K. Roeher, A. von Sandersleben, S. Diedrichs, H. Reichenspurner, A.E. Goetz, D.A. Reuter, Individually optimized hemodynamic therapy reduces complications and length of stay in the intensive care unit: a prospective, randomized controlled trial, Anesthesiology 119 (2013) 824–836.

[39] B. Wu, J. Chen, Y. Yang, Biomarkers of acute kidney injury after cardiac surgery: a narrative review, Biomed. Res. Int. 2019 (2019) 7298635.

[40] D. Zhou, Y. Li, L. Lin, L. Zhou, P. Igarashi, Y. Liu, Tubule-specific ablation of endogenous β-catenin aggravates acute kidney injury in mice, Kidney Int. 82 (5) (2012) 537–547.

[41] H.U. Zacharias, J. Hochrein, F.C. Vogl, G. Schley, F. Mayer, C. Jeleazcov, K.-U. Eckardt, C. Willam, P.J. Oefner, W. Gronwald, Identification of plasma metabolites prognostic of acute kidney injury after cardiac surgery with cardiopulmonary bypass, J. Proteome Res. 14 (7) (2015) 2897–2905.

[42] J.A. Davidson, B.S. Frank, T.T. Urban, M. Twite, J. Jaggers, L. Khailova, J. Klawitter, Serum metabolic profile of postoperative acute kidney injury following infant cardiac surgery with cardiopulmonary bypass, Pediatric Nephrol. 36 (10) (2021) 3259–3269.

[43] A. De Luca, S. Pierno, D.C. Camerino, Taurine: the appeal of a safe amino acid for skeletal muscle disorders, J. Transl. Med. 13 (2015) 243.

[44] I. Adedara, S. Alake, L. Olajide, M. Adeyemo, T. Ajibade, E. Farombi, Taurine ameliorates thyroid hypofunction and renal injury in L-NAME-induced hypertensive rats, Drug Res. (Stuttg) 69 (02) (2019) 83–92.

[45] Y.S. Kim, S.H. Sung, Y. Tang, E.J. Choi, Y.J. Choi, Y.J. Hwang, P.J. Park, E.K. Kim, Protective effect of taurine on mice with doxorubicin-induced acute kidney injury, Adv. Exp. Med. Biol. 975 (Pt 2) (2017) 1191–1201.

[46] X. Wan, XinHua Li, Q. Wang, B. Zheng, C. Zhou, X. Kang, D. Hu, H. Bao, A.i. Peng, Metabolitic profiling of amino acids in paraquat-induced acute kidney injury, Clin. Exp. Nephrol. 23 (4) (2019) 474–483.

[47] J. Sun, M. Shannon, Y. Ando, L.K. Schnackenberg, N.A. Khan, D. Portilla, R. D. Beger, Serum metabolomic profiles from patients with acute kidney injury: a pilot study, J. Chromatogr. B Analyt. Technol. Biomed. Life Sci. 893-894 (2012) 107–113.

[48] Y.-Y. Zhao, X.-L. Cheng, F. Wei, X.-Y. Xiao, W.-J. Sun, Y. Zhang, R.-C. Lin, Serum metabonomics study of adenine-induced chronic renal failure in rats by ultra performance liquid chromatography coupled with quadrupole time-of-flight mass spectrometry, Biomarkers 17 (1) (2012) 48–55.

[49] W. Han, L. Li, Evaluating and minimizing batch effects in metabolomics, Mass Spectrometry Rev. (2020) online ahead of print.

[50] J. Ma, T. Chen, S. Wu, C. Yang, M. Bai, K. Shu, K. Li, G. Zhang, Z. Jin, F. He, H. Hermjakob, Y. Zhu, iProX: an integrated proteome resource, Nucl. Acids Res. 47 (2019) D1211–D1217.